Electronic Supplementary Material (ESI) for Journal of Materials Chemistry A.

Formulating electronic descriptors to rationally design graphene-supported single-atom catalysts for oxygen electrocatalysis

*Jungwoo Choi[1], Doosun Hong[1], and Hyuck Mo Lee[1] **

[1]Department of Materials Science and Engineering, Korea Advanced Institute of Science and Technology (KAIST), Daejeon 34141, Republic of Korea.

*corresponding author, email: hmlee@kaist.ac.kr

KEYWORDS: Oxygen electrocatalysis, Single-atom catalysts, Density functional theory, Electronic structure, Descriptor

SUPPORTING INFORMATION

Selection of physical quantities representing the catalytic performance

To investigate the origin of the catalytic performance from the electronic structure of G-SACs using DFT, we focused on the adsorption energy of oxygen (ΔE_O) and the binding energy of a single atom (E_{bind}) as physical quantities to represent the catalytic activity and stability, respectively. Previous studies have shown that the ORR of G-SACs proceeds through a $4e^-$ transfer pathway, as is given by Equations (1–4).[1, 2]

$$O_2 + H^+ + e^- + * \rightarrow OOH^* \quad (1)$$

$$OOH^* + H^+ + e^- \rightarrow O^* + H_2O \quad (2)$$

$$O^* + H^+ + e^- \rightarrow OH^* \quad (3)$$

$$OH^* + H^+ + e^- \rightarrow H_2O + * \quad (4)$$

where * denotes an adsorbed state on the active site. The Gibbs free energy changes for each step were described as the adsorption energy of the O, OH, and OOH intermediates. Therefore, the overpotential representing the catalytic activity could be evaluated by the adsorption energy of each intermediate. In addition, the adsorption energies of the intermediates at the single active site are in a scaling relation with each other; thus, the activity of the catalyst can be described with only the ΔE_O, which ensures the reliability of the selection of ΔE_O as a physical quantity to represent the catalytic activity. The ΔE_O is calculated using Equation (5).

$$\Delta E_O = E_{O*} - (E_{H_2O} - E_{H_2}) - E_{substrate} \quad (5)$$

where E_{O*}, E_{H_2O},, E_{H_2}, and $E_{substrate}$ represent the total energy of oxygen-adsorbed G-SACs, H_2O, H_2 molecules in the gas phase using the approaches outlined by Norskov et al.,[3] and the

graphene-based substrate, respectively. We selected the binding energy of the single atom (E_{bind}) as a physical quantity to represent the catalytic stability, and it is calculated using Equation (6).

$$E_{bind} = E_{SACs} - E_{substrate} - E_{SA} \quad (6)$$

where E_{SACs}, $E_{substrate}$, and E_{SA} represent the total energy of the G-SACs, graphene-based substrate, and a single metal atom referenced to their metallic states, respectively. The strong binding energy of the single atom indicates a strong resistance to agglomeration and dissolution of single atoms owing to their high chemical potential in harsh operating environments.

Details about calculating orbital center and vaccum electrostatic potential corrected Fermi energy level.

The orbital energy levels of individual orbitals were represented by calculating the orbital center. The orbital center was calculated as follows,

$$Orbital\ center = \frac{\int E_{\times} D(E) dE}{\int D(E) dE}$$

where D(E) is the PDOS of the single atom in G-SACs. The FO is selected by the maximum value of each orbital center.

The Fermi energy of each system was calculated as follows,

$$E_F = E_F^{DFT} - E_{Vacuum}^{DFT}$$

where E_F^{DFT} is the DFT calculated Fermi energy and E_{Vacuum}^{DFT} is the averaged electrostatic energy level in the vacuum.

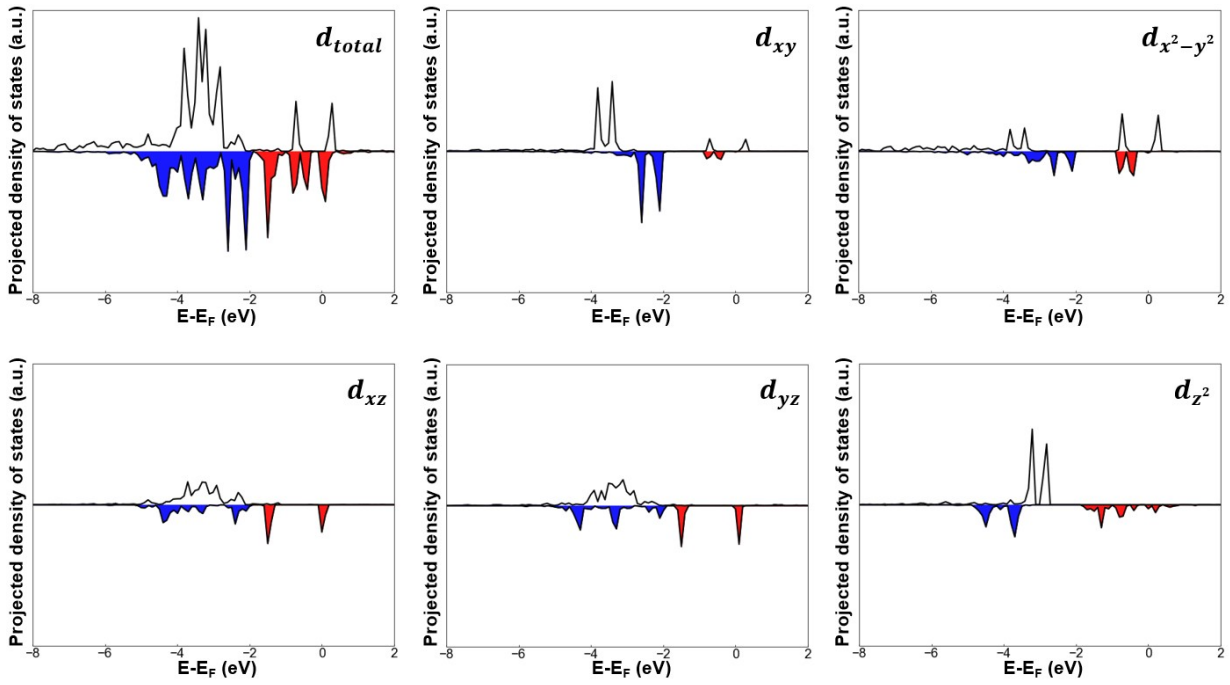

Figure S1. PDOS for the 3d hybrid orbital and the $3d_{xy}$, $3d_{x^2-y^2}$, $3d_{xz}$, $3d_{yz}$, and $3d_{z^2}$ orbitals of Cu–N–C. The upper and lower lines mean the PDOS before and after oxygen interaction, respectively. The red and blue regions represent the antibonding and bonding states, respectively, after interacting with oxygen.

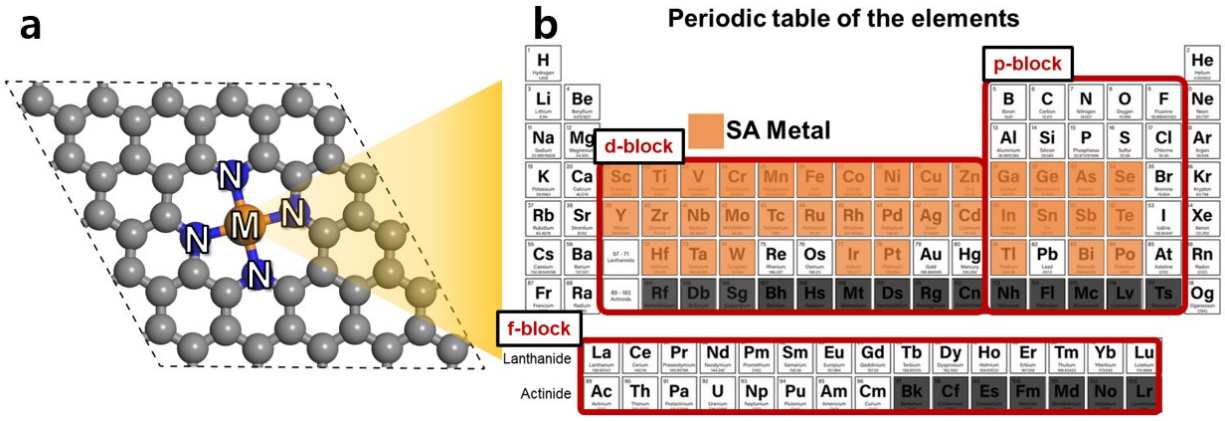

Figure S2. Schematic illustration of the G-SACs examines in this work. (a) Structure of G-SACs, in which C, N, and the single atom are shown in black, blue, and orange, respectively. (b) All 36 elements that we explored as single atoms in this work.

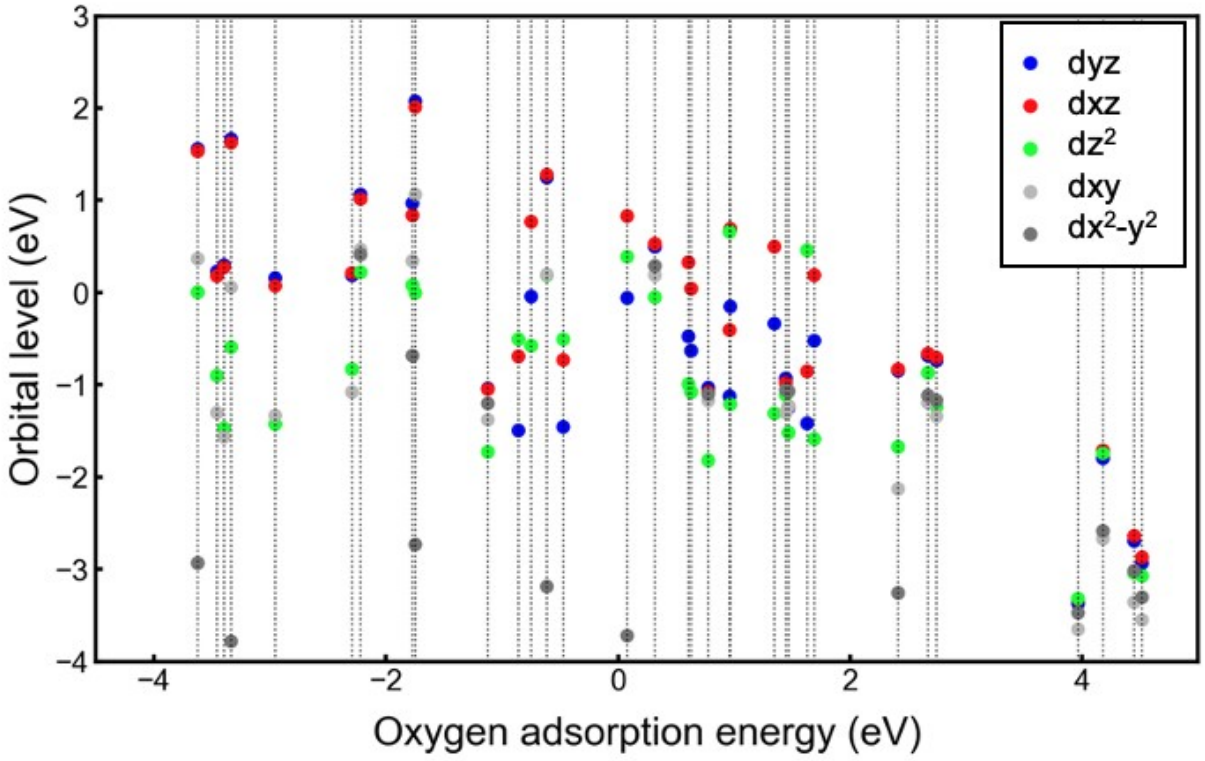

Figure S3. Calculated PDOS centers versus the corresponding values of ΔE_O for the G-SACs.

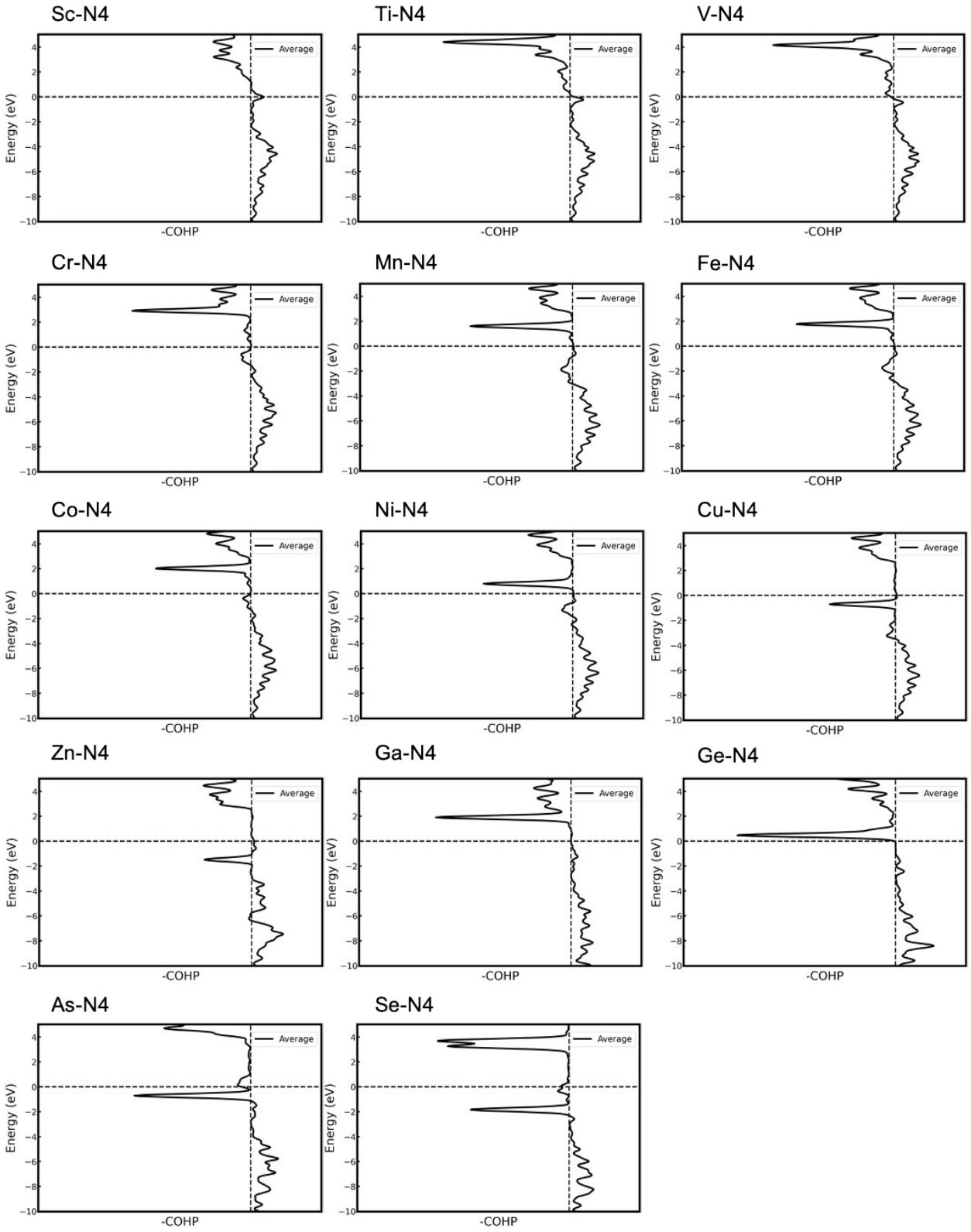
Sc-N4
Ti-N4
V-N4
Cr-N4
Mn-N4
Fe-N4
Co-N4
Ni-N4
Cu-N4
Zn-N4
Ga-N4
Ge-N4
As-N4
Se-N4
Average
Energy (eV)
-COHP

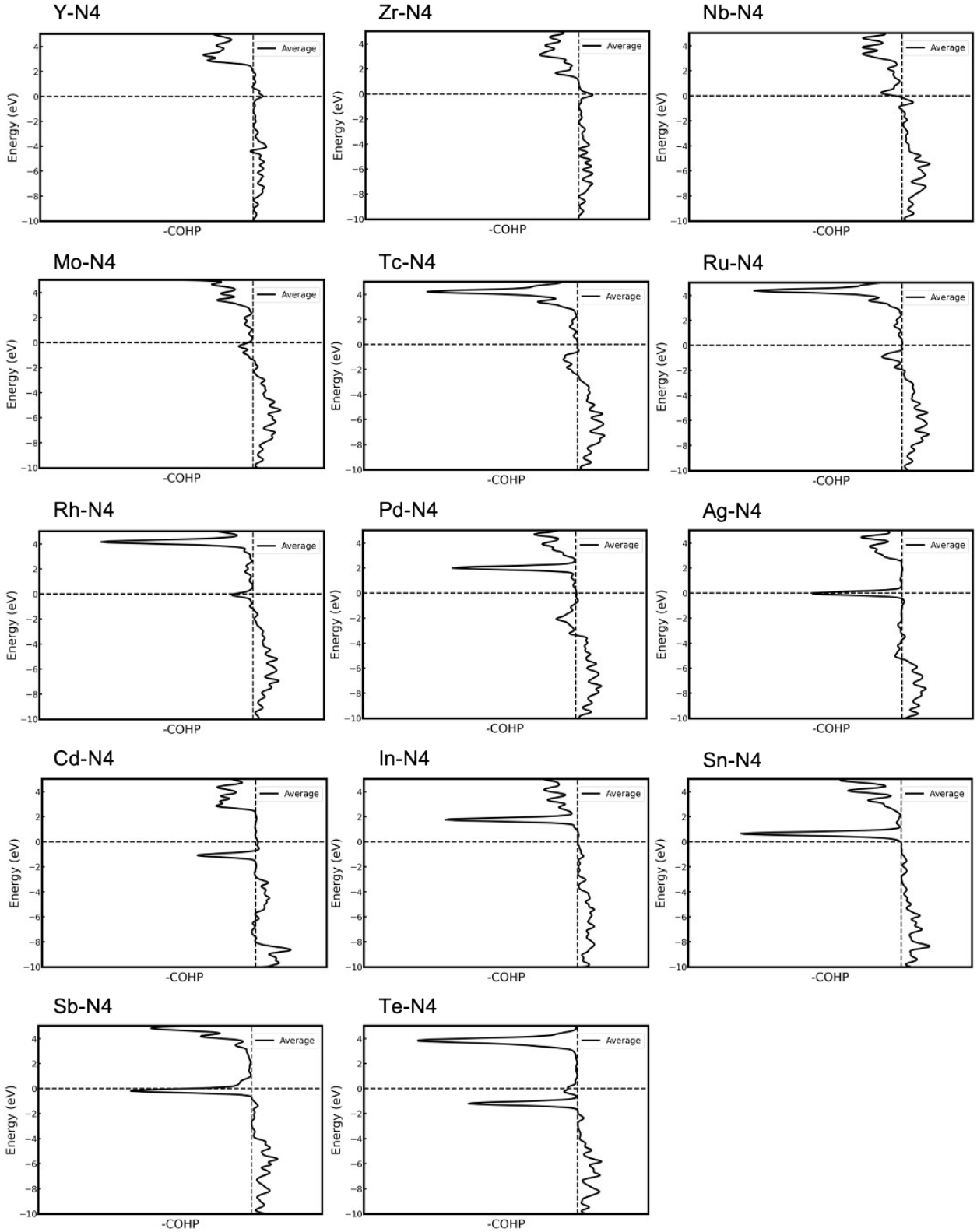
Y-N4
Zr-N4
Nb-N4
Mo-N4
Tc-N4
Ru-N4
Rh-N4
Pd-N4
Ag-N4
Cd-N4
In-N4
Sn-N4
Sb-N4
Te-N4
Average
Energy (eV)
-COHP

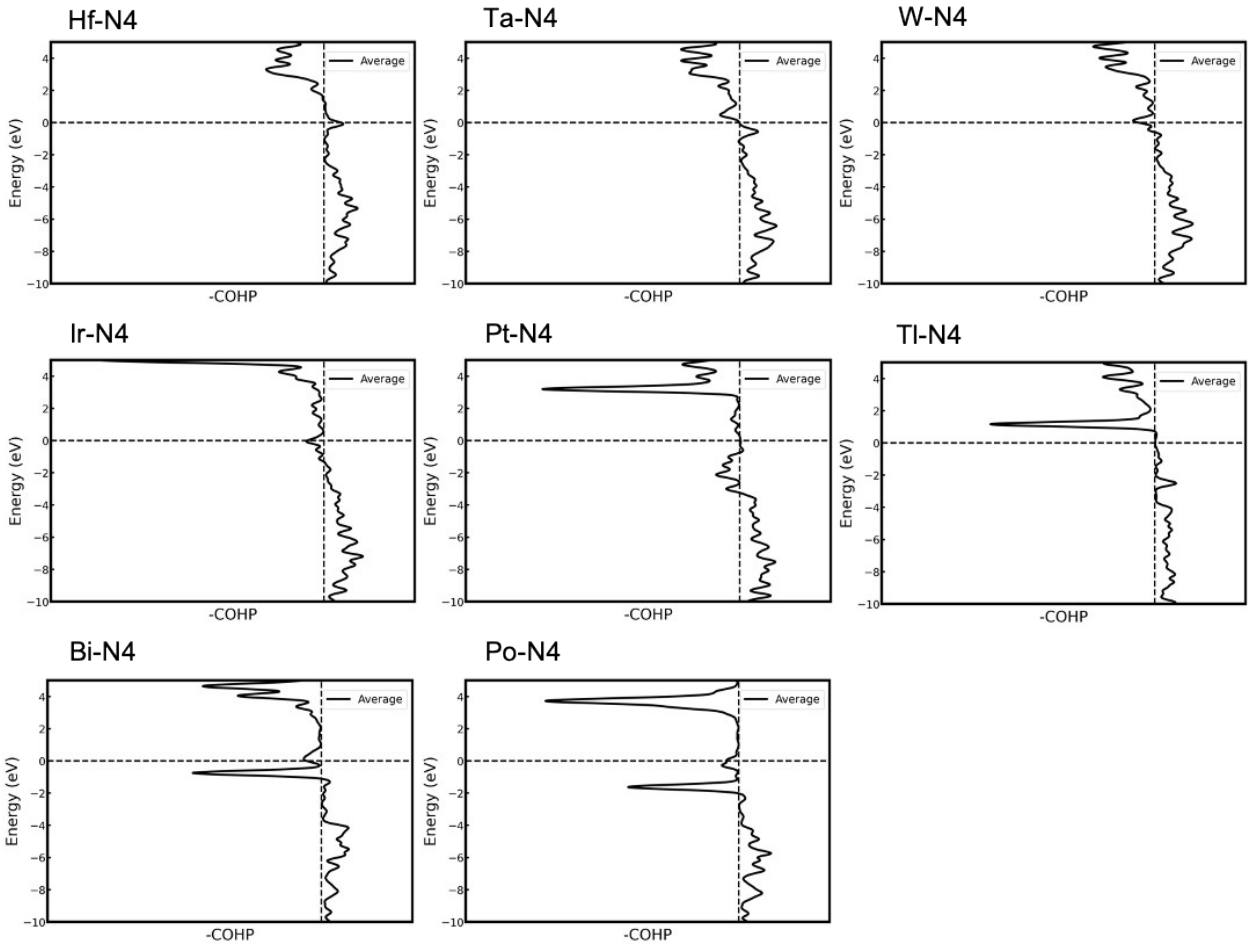

Figure S4. COHP bonding analysis between single atom and N4 for the 36 G-SACs. The dotted vertical and horizontal lines represent lines where –COHP is a value of 0 and E-E_F is value of 0, respectively.

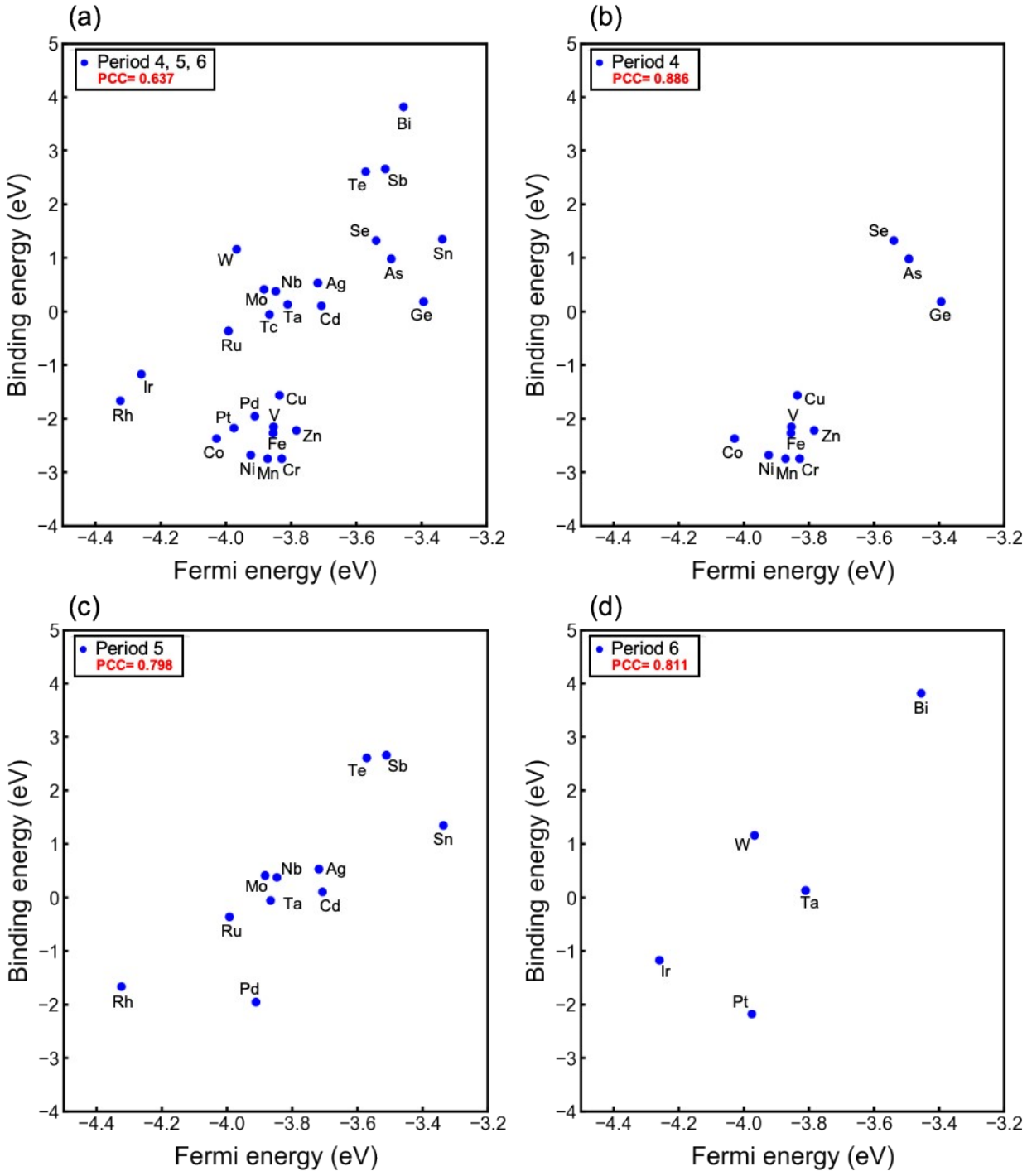

Figure S5. Calculated E_{bind} of single atoms against the corresponding value of Fermi level for G-SACs of each period element.

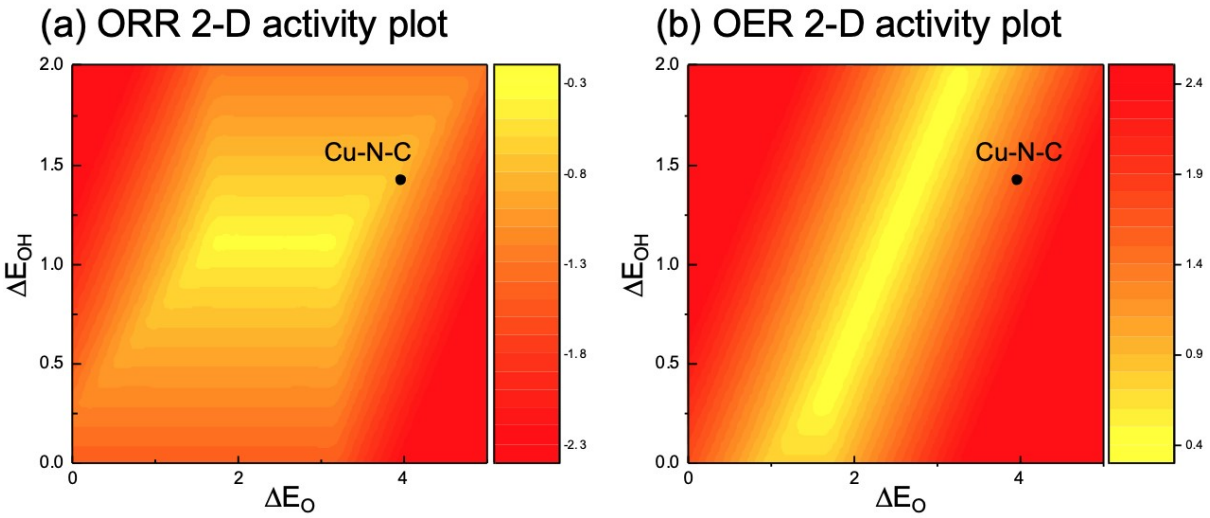

Figure S6. Trend of the catalytic activity is expressed as a function of the O (x-axis) and OH (y-axis) adsorption energies at 1.23 V versus the RHE. The z-axis shows the calculated activity. (a) and (b) represent the 2-D activity plot for ORR and OER, respectively.

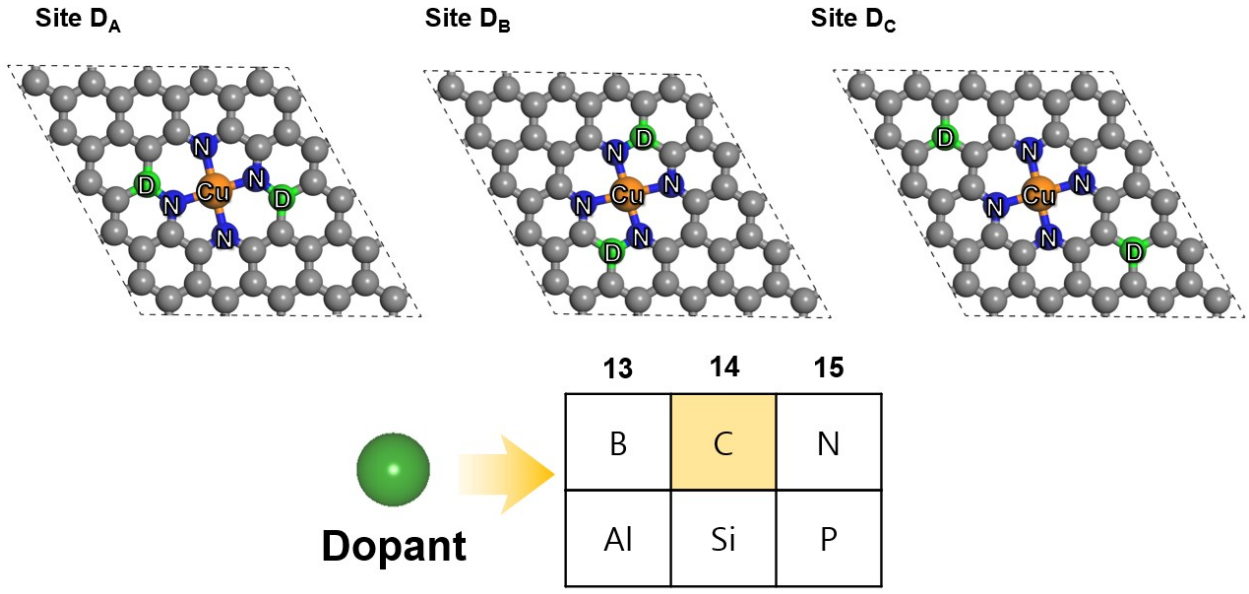

Figure S7. Schematic illustration of dopant-tuned Cu–N–C, in which C, N, the dopant, and Cu are shown in black, blue, green, and orange, respectively. Three possible doping sites near Cu–N_4 are considered, which are named D_A, D_B, and D_C,. The p-block elements B, C, N, Al, Si, and P are considered as dopants. O, F, S, and Cl are excluded owing to the large structural changes they induce.

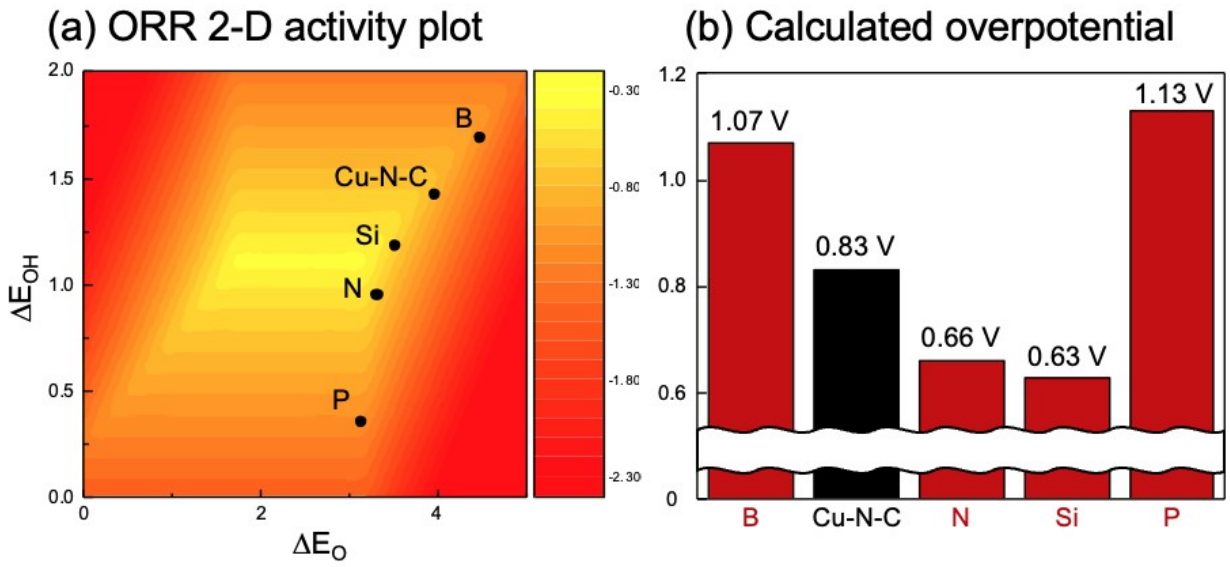

Figure S8. Calculated activity for ORR of doped Cu-N-C systems. (a) Trend of the catalytic activity is expressed as a function of the O (x-axis) and OH (y-axis) adsorption energies at 1.23 V versus the RHE. The z-axis shows the calculated activity. (b) DFT calculated overpotential of doped Cu-N-C systems. The black bar and red bar represent Cu-N-C and doped Cu-N-C systems, respectively. The B, N, Si, and P mean the dopants. The Al doped Cu-N-C is excluded because this system renders more stable OH adsorption on the Al site than on the Cu site.

	E_{DFT} (eV)		
Dopants	**Site D_A**	**Site D_B**	**Site D_C**
B	-417.74	-417.00	-415.81
C	-421.08	-421.08	-421.08
N	-415.56	-416.48	-416.98
Al	-404.89	-401.93	-400.03
Si	-410.46	-407.85	-407.49
P	-409.23	-407.61	-407.70

Table S1. Relative stability of each site for six dopants. In all dopants except N, the D_A site was confirmed to be the most stable.

REFERENCES

1. C. Zhang, J. Sha, H. Fei, M. Liu, S. Yazdi, J. Zhang, Q. Zhong, X. Zou, N. Zhao and H. Yu, *Acs Nano*,

2017, **11**, 6930-6941.

2. J. Zhang, Y. Zhao, C. Chen, Y.-C. Huang, C.-L. Dong, C.-J. Chen, R.-S. Liu, C. Wang, K. Yan and Y. Li, *Journal of the American Chemical Society*, 2019, **141**, 20118-20126.
3. J. K. Nørskov, J. Rossmeisl, A. Logadottir, L. Lindqvist, J. R. Kitchin, T. Bligaard and H. Jonsson, *The Journal of Physical Chemistry B*, 2004, **108**, 17886-17892.